

# Hydrodynamic Flow Characteristics in an Internally Circulating Fluidized Bed Gasifier

**J. P. Simanjuntak**

Mechanical Engineering Department,  
State University of Medan,  
Medan 20221, North Sumatera, Indonesia  
e-mail: janterps@gmail.com

**K. A. Al-attab<sup>1</sup>**

School of Mechanical Engineering,  
Universiti Sains Malaysia,  
Engineering Campus,  
Nibong Tebal 14300, Penang, Malaysia  
e-mail: khaledalattab@yahoo.com

**Z. A. Zainal**

School of Mechanical Engineering,  
Universiti Sains Malaysia,  
Engineering Campus,  
Nibong Tebal 14300, Penang, Malaysia  
e-mail: mezainal@usm.my

*In this paper, the hydrodynamic flow inside an internally circulating fluidized bed (ICFBG) was characterized using experimental and three-dimensional computational fluid dynamics (CFD) models. Eulerian-Eulerian model (EEM) incorporating the kinetic theory of granular flow was implemented in order to simulate the gas–solid flow. A full-scale plexiglass cold flow experimental model was built to verify simulation results prior to the fabrication of the gasifier. Six parameters were manipulated to achieve the optimum design geometry: fluidization flow rate of the draft tube ( $Q_{dt}$ ), aeration flow rate of the annulus ( $Q_{an}$ ), initial bed static height ( $H_{bs}$ ), draft tube height ( $H_{dt}$ ), draft tube diameter ( $D_{dt}$ ), and orifice diameter ( $D_{or}$ ). The investigated parameters showed strong effect on the particle flow characteristics in terms of the pressure difference ( $\Delta P$ ) and solid circulation rate ( $G_s$ ). The predicted results by simulation for the optimum case were in close agreement with experimental measurements with about 5% deviation. The results show that the ICFBG operated stably with the maximum  $G_s$  value of 86.6 kg/h at  $Q_{dt}$  of 350 LPM,  $Q_{an}$  of 150 LPM,  $H_{bs}$  of 280 mm,  $H_{dt}$  of 320 mm,  $D_{dt}$  of 100 mm, and  $D_{or}$  of 20 mm. [DOI: 10.1115/1.4041092]*

*Keywords: internally circulating fluidized bed, solid circulation rate, Eulerian-Eulerian model, kinetic theory of granular flow*

## Introduction

Biomass with its neutral effect in greenhouse emissions is commonly cofired with coal in the medium- and large-scale power plants and utilized in boilers in single-stage combustion to reduce carbon footprint. However, research showed that biomass with high chlorine content produces hydrogen chloride that causes erosion for the boiler tubes when directly burned under high temperature in fixed bed reactors [1]. Fluidized bed combustors are widely used in solid fuels utilization with long residence time and efficient combustion [2]. Several other techniques have been recently developed to enhance the combustion of lower heating value fuels. Chemical looping combustion was initially developed to enhance combustion efficiency but also used recently in CO<sub>2</sub> capture technology [3,4]. Other technique such as the catalytic combustion has been widely investigated [5,6]. One of the convenient ways to get heat from biomass is through the direct combustion of syngas after an updraft gasifier without the necessity of syngas treatment and tar removal [7].

One of the main downsides in fixed bed gasifiers is the nonuniform heat and mass transfer between biomass and oxidizer that makes a steady-state operation not attainable with constant fluctuation in syngas quality. On the other hand, cyclone gasifiers operate at steady-state with stable syngas quality [8]. Bubbling fluidized bed gasifiers overcome this issue by the excellent solid–gas contact and mixing with continuous fuel feeding that result in an improved and consistent quality of syngas [9,10]. Further enhancement in mixing quality and heat transfer, hence, gasification efficiency and syngas quality was achieved by the external circulation of the materials in circulating fluidized bed gasifiers (CFBG) although at the expense of higher initial and operation cost [11].

Internally circulating fluidized bed gasifier (ICFBG) is a modified type of CFBG but in a more compact and cost-effective form. The fluidized bed is divided by a tube or baffle plates into two separate gasification and combustion where heat is transferred from the combustion zone to the gasification zone by the circulation of hot solid bed materials. Thus, the internal circulation of heat with less exposed surface area provides lower heat losses and higher efficiency. Another advantage of the ICFBG reactor is the higher process residence time resulting in a higher syngas quality comparable to CFBG but in more compact form and lower initial cost.

One of the earlier configurations of ICFBG known as the clapboard-type comprises a rectangular cross section reactor with single separator plate or baffle separates gasification and combustion zones [12]. Different types of gasification agents were experimentally tested such as steam [13] and steam/oxygen mixtures [14], while air is used for the combustion. Another well-known ICFBG configuration comprises coaxial cylindrical vessels mounted vertically on top of each other with a central draft tube where gasifier chamber is at the bottom and combustion chamber is at the top [15,16]. Modified annulus geometry with simpler design and less components compared to the previous type was also experimentally investigated. The design comprises two concentric tubes with circular [17] or square cross section [18]. This design reduces the required height of the reactor and fabrication cost considerably.

The performance of ICFBG depends mainly on the heat transfer quality between combustion and gasification zones. Therefore, the vast majority of research in this area is dedicated to study the hydrodynamic flow characteristics inside the reactor and the solid circulation rate and the ways to improve it. The use of experimental cold-flow model is an important and low-cost tool to investigate the circulation mechanism inside the reactor and the effect of operating variables on circulation. However, only operating conditions can be varied to characterize the flow with very limited access to the geometry variables and their effect on the flow. On the other hand, numerical modeling and computational fluid dynamic (CFD) simulation have the advantage of unlimited access

<sup>1</sup>Corresponding author.

Contributed by the Advanced Energy Systems Division of ASME for publication in the JOURNAL OF ENERGY RESOURCES TECHNOLOGY. Manuscript received January 24, 2018; final manuscript received July 22, 2018; published online September 14, 2018. Assoc. Editor: Reza Sheikhi.

**Table 1 Simulation setup and gas–solid properties**

Parameters	Value
Particle density ( $\rho_p$ )	1520 (kg/m <sup>3</sup> )
Gas density ( $\rho_g$ )	1.2 (kg/m <sup>3</sup> )
Gas viscosity ( $\mu$ )	$1.79 \times 10^{-5}$ (Pa·s)
Time step used ( $\Delta t$ )	0.001(s)
Outlet condition ( $P$ )	101,325 (Pa)
Particle diameter ( $d_p$ )	450 ( $\mu$ m)
Fluidizing flow rate ( $Q_{dt}$ )	300, 350, 400, 450 (LPM)
Aeration flow rate ( $Q_{an}$ )	50, 100, 150, 200, 250 (LPM)
Initial bed height ( $H_{bs}$ )	260, 280, 300, 320 (mm)
Draft tube height ( $H_{dt}$ )	260, 280, 300, 320 (mm)
Draft tube diameter ( $D_{dt}$ )	75, 100, 125, 150 (mm)
Orifice diameter ( $D_{or}$ )	10, 15, 20, 25 (mm)
Solid volume fraction	0.63

to all variables at a relatively lower cost. However, simulation programs are limited with the computational demand and capacity, and also the need for result verification and validation.

The hydrodynamic flow was studied using cold-flow experimental models covering wide range of reactor geometries such as square [18] and circular [19,20] annulus/draft tube and clapboard-type with single [21] and double baffle plates [22]. As for the CFD modeling, two major approaches are commonly used to predict the bed particles behavior during the fluidization and circulation: the Eulerian-Eulerian model (EEM) and discrete element method [23,24]. Majority of the CFD simulation studies focused on the rectangular reactor geometry with baffle plates either with discrete element method [24] or EEM [25] approaches. Other modeling approaches were also investigated such as multiphase particle-in-cell method [22], two-fluid finite volume with SIMPLEX algorithm [26], and kinetic theory of granular mixture [27,28].

In this paper, CFD model was developed to characterize the hydrodynamic cold flow inside ICFBG in order to determine the optimum design geometry of the reactor. EEM and kinetic theory of granular mixture simulation approaches were utilized to simulate the solid–gas flow and the effects of various operating parameters on the flow were assessed. Simulation results were verified using cold flow experimental modeling.

### Internally Circulating Fluidized Bed Gasifier Theory

This type of gasifier is also often referred to as the dual fluidized bed gasifier since the gasification and combustion zones are separated in two chambers. Therefore, syngas heating value from the gasification chamber is increased by reducing the inert diluents ( $N_2 + CO_2$ ) concentration since the combustion zone is separated. The operation theory of the ICFBG is fundamentally different from the conventional gasifiers since the heat required for gasification is supplied indirectly. In general, the indirect heat supply could be provided by external source like plasma, solar or other sources, or through the internal recirculation of bed material and char between two separate combustion and gasification zones. Gasification occurs in the outer shell or annulus tube, while combustion is in the central zone known as the draft tube. Biomass material is fed to the annulus tube with a mild supply of gasification air in a process known as aeration flow ( $Q_{an}$ ) which is

commonly not enough to create fluidization in the bed materials. On the other hand, combustion air or fluidization flow ( $Q_{dt}$ ) is supplied at the bottom of the draft tube. Solid materials are circulated between the annulus and draft tubes mainly by the aid of  $Q_{an}$  and  $Q_{dt}$  flows. Hot sand along with some of the char created in the annulus (gasification zone) are pushed to the draft tube (combustion zone) through circular holes (orifice) at the bottom of the tube, while fluidization motion causes hot sand to overflow from the top of draft tube back to the annulus. Other factors that can also affect the solid circulation rate ( $G_s$ ) are initial bed static height ( $H_{bs}$ ), draft tube height ( $H_{dt}$ ), draft tube diameter ( $D_{dt}$ ), and orifice diameter ( $D_{or}$ ). The mix between exhaust gas and syngas is prevented by directing the exhaust through additional tube known as the dipleg.

**Computational Fluid Dynamics Simulation.** A three-dimensional geometry representing the internal circulation part of the ICFBG reactor was created and meshed using GAMBIT software version 2.4.6. Tet/Hybrid elements were used for meshing and the results of mesh independence study showed that increasing the mesh size by reducing mesh spacing in the range of 1–0.1 mm did not yield any noticeable difference in the flow characteristics. The final number of elements was set to 447,160. The two annulus and draft tube beds were connected via eight orifices placed 80 mm above the air distributor. Fluidization air was supplied through velocity input plate at the bottom of the draft tube, while a conical plate with an inclined angle of 60 deg was used for aeration supply to the annulus.

The simulation was performed using FLUENT 6.3 CFD simulation program. The main purpose of the simulation was to investigate the effect of different operating and design parameters on the hydrodynamic characteristics of the gas–solid flow. Main manipulated variables were  $Q_{dt}$ ,  $Q_{an}$ ,  $H_{bs}$ ,  $H_{dt}$ ,  $D_{dt}$ , and  $D_{or}$ , while the main response variables were  $G_s$ , bed pressure, and pressure difference between annulus and draft tube. Pressure profile was also investigated since pressure levels fluctuate periodically with time as a result of the bubbling fluidization process. Second-order upwind discretization was used for both momentum and volume fraction solutions. The typical simulation domain, variables setup, and gas–solid properties are shown in Table 1.

The CFD simulation was divided into six groups based on the manipulated variables as shown in Table 2. In these groups, only one parameter was varied while fixing the other parameters. However, for better understanding on the combined effect of geometry and operating variables, the effect of  $Q_{an}$  was also added to the geometry effect simulation groups 3–6 while keeping  $Q_{dt}$  at the optimum value of 350 LPM.

Eulerian-Eulerian model with the kinetic theory of granular flow is a common model to predict the fluidization motion of particles in fluidized bed reactors. A first-order upwind discretization scheme was used for momentum and continuity equations were solved for each phase, where the momentum equations are linked equations while the quadratic upwind interpolation scheme was used for the volume fraction equations. A time-step of 0.001 s was used to advance the solution in time with a second-order implicit time integration scheme.

The bed material circulation rate through the orifice was calculated by Eq. (1):

**Table 2 CFD simulation groups based on manipulated variables**

Group no.	$Q_{dt}$ (LPM)	$Q_{an}$ (LPM)	$H_{bs}$ (mm)	$D_{dt}$ (mm)	$D_{or}$ (mm)	$H_{dt}$ (mm)
1	300, 350, 400, 450	150	280	100	20	320
2	350	50, 100, 150, 200, 250	280	100	20	320
3	350	50, 100, 150, 200, 250	260, 280, 300, 320	100	20	320
4	350	50, 100, 150, 200, 250	280	75, 100, 125, 150	20	320
5	350	50, 100, 150, 200, 250	280	100	10, 15, 20, 25	320
6	350	50, 100, 150, 200, 250	87.5% of $H_{dt}$	100	20	260, 280, 350, 370

$$G_s = (1 - \varepsilon_f) \rho_s U_{s,av} A_o \quad (1)$$

where  $\varepsilon_f$ ,  $U_{s,av}$ ,  $\rho_s$ , and  $A_o$  are the voidage in the orifice, the solid density, the average solid velocity magnitude through the orifices, and the orifice area, respectively. A new parameter that provides a good prospect of the combined effect of fluidization and aeration flows is the air flow ratio ( $R_Q$ ).  $R_Q$  was calculated by Eq. (2) as the ratio of the air aeration to the air fluidization flow rates

$$R_Q = Q_{an}/Q_{dt} \quad (2)$$

**Experimental Model Setup.** An experimental full-scale Plexi-glass model was developed based on the optimum geometry obtained from the CFD simulation. The aim is to study the hydrodynamic flow of gas–solid flow through the visual inspection of the flow behavior with the main focus on  $G_s$  and static pressure measurements. The results were also used to validate the results obtained from the CFD simulation. A schematic diagram of the experimental model setup is illustrated in Fig. 1(a). The main cylinders of the annulus, draft tube, and a dipleg were made of Plexi-glass. The annulus has a 0.30 m inner diameter and 0.70 m height with a central draft tube of 0.1 m inner diameter and 0.32 m height. Eight orifices of 0.02 m diameter were drilled in the draft tube wall 0.08 m above the distributor plate. The experimental setup resembles the optimum reactor geometry in simulation groups 1 and 2. The other parts included mild steel plate and conical air distributors with bubble caps shown in Fig. 1(b) for draft tube and annulus, respectively, with mild steel air inlet ducts being used in the experimental test of the ICFBG. Each bubble cap contained four air injectors of 0.0025 m diameter.

A 1.5 kW ring-type air blower was used for the air supply with two rotameters and valves to measure and control the fluidization and aeration flow rates which were varied in the range of 300–450 LPM and 50–250 LPM, respectively, with 50 LPM intervals. A metal screen was used to collect the bed particle that overflows from the draft tube section for  $G_s$  measurement which was

determined by collecting solids that overflows from the top of the draft tube on the metal screen for a known interval of time and weighing to obtain the bed material circulation rate. Two U-tube manometers were used to measure the static pressure at the fluidization and aeration air distributors. The bed was filled with Geldart group B silica sand particles with a mean diameter of 450  $\mu\text{m}$  and a density of 1520  $\text{kg/m}^3$ . The draft tube was operated in the bubbling fluidization regime with superficial velocity below 1 m/s, while the annulus was operated in fixed or moving bed mode with superficial velocity below the minimum fluidization velocity, thus, the circulation of bed material was caused by the particles overflow from the draft tube section.

**Hydrodynamic Gas-Solid Circulation Mechanism.** Both CFD simulation and experimental models were utilized to gain a better understanding of the mechanism of hydrodynamic gas–solid circulation between annulus and draft tube. Simulation group 1 with  $Q_{dt}$  of 350 LPM as the optimum case was considered in this section to discuss the material circulation phenomena between annulus and draft tube zones. The orifice effect has resulted in a significant pressure drop inside the draft tube. The average static pressure magnitude at 30 s of running was plotted in Fig. 2(a) for the horizontal X–Z plane at the orifice holes. Pressure drop inside the draft tube resulted in a considerable pressure difference between the annulus and draft tube zones. This is due to the higher solid volume fraction in the annulus compared to the draft tube which moved the solid from the annulus to the draft tube. On the other hand, bed pressure started to elevate inside the draft tube along the Y-axis toward the top of the tube exceeding the bed pressure inside the annulus zone as illustrated in Fig. 2(b). This has caused the bed material to overflow back to the annulus zone completing the flow circulating process.

Another important factor that affected material circulation was the bubbling effect. Figure 2(c) plots the average value of the bed pressure against time in the annulus and the draft tube zones along the X–Z plate at the orifice. The periodic vigorous bubbling of the bed materials inside the draft tube leads to fluctuations in the bed

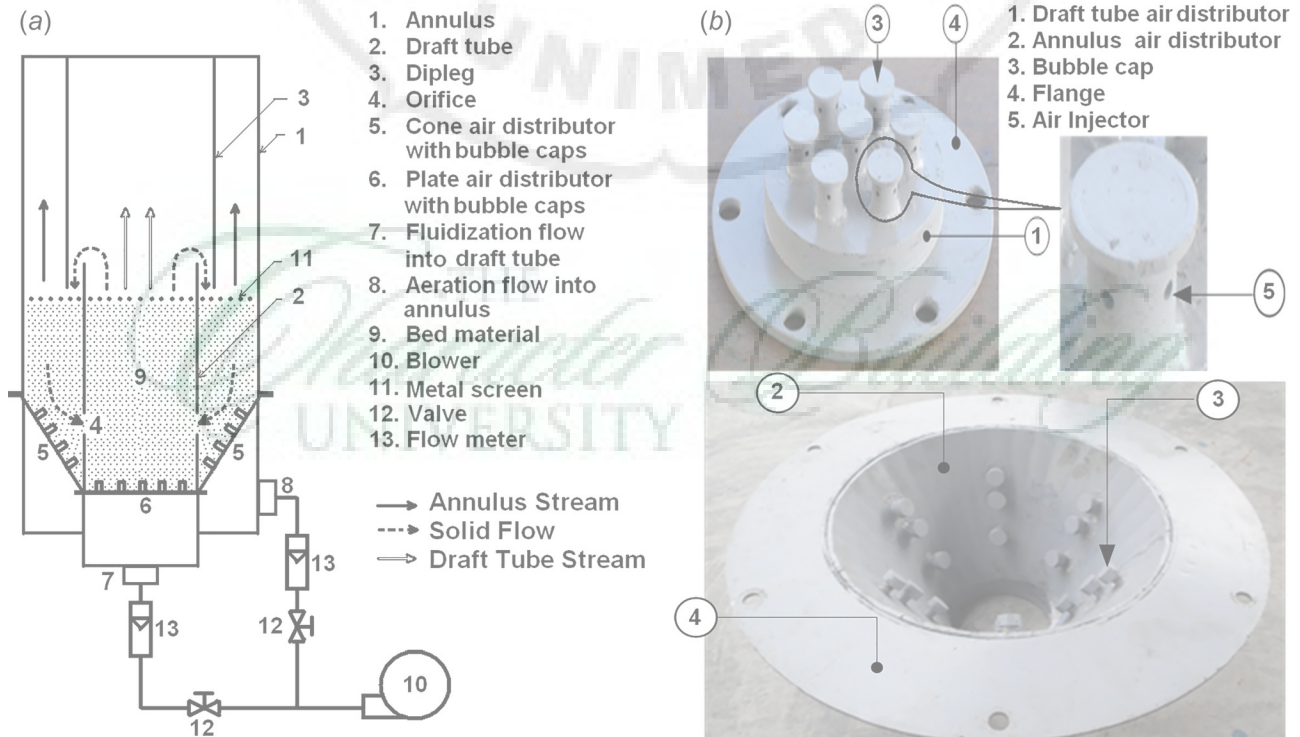


Fig. 1 (a) Configuration of the reactor geometry of the model and experimental setup and (b) annulus and draft tube air distributors

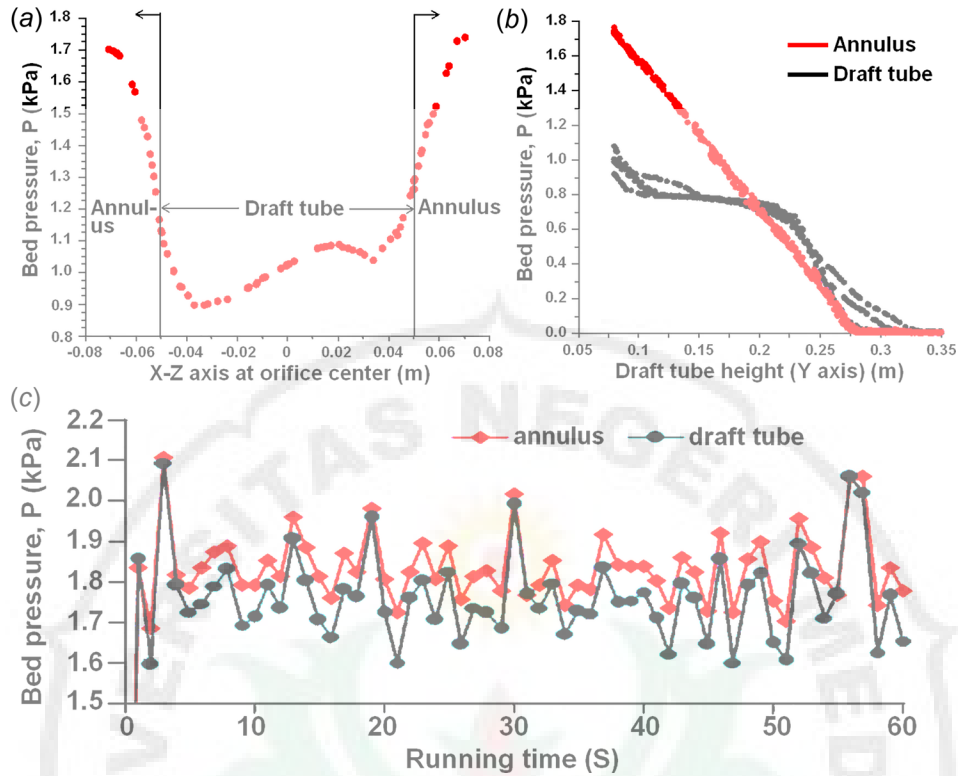


Fig. 2 Bed pressure for simulation group 1 at Qdt: 350 LPM Along: (a) radial axis (X–Z axis) through the orifice center, (b) draft tube height (Y-axis), and (c) orifice center (X–Z axis)

pressure. Through the entire test period, the pressure in the annulus was higher than that in the draft tube, thus, providing the driving force for solid flow from the annulus to draft tube through orifice holes. After an initial period of about 4 s, the flow hydrodynamics in the bed stabilized, resulting in a fixed pressure fluctuation pattern with time. This pressure fluctuation is essential to overcome the static friction between bed particles providing continuous gas–solid circulation.

For better understanding of the bed material circulation phenomena, the optimum fluidization flow of 350 LPM was compared with the other flow rates. Instantaneous spatial distributions contours of the bed material based on solid volume fraction are shown in Fig. 3. Four fluidization rates in the range of 300–450 LPM representing simulation group 1 shown earlier in Table 2 were compared. Initially, the bed material filled both the annulus and the draft tube regions at the same initial level 280 mm above the distributor plate. Aeration flow into the annulus was maintained constant at 150 LPM. The changes in volume fraction of the bed material are significant inside the draft tube unlike the annulus zone. This indicated a vigorous fluidization regime inside the draft tube with a bed height expansion due to the high fluidization air flow. On the other hand, the aeration flow was below the minimum flow required for bed material fluidization.

As the draft tube was fluidized at  $Q_{dt}$  higher than  $Q_{an}$ , the fluidization regime in the draft tube changed from fixed bed regime to bubbling regime as represented by the presence of voids (i.e., extreme low solid concentration). At 300 LPM  $Q_{dt}$ , no voids were observed in the annulus as the low aeration flow caused no bubbling in the annulus which is commonly known as the fixed bed regime. The fluidization in the draft tube was not sufficient to mix and expand the bed material above the top of the draft tube. Therefore, bed material overflow from the draft tube into the annulus was low resulting in low circulation.

Increasing the fluidization flow to the draft tube up to 350 LPM resulted in a vigorous fluidization regime. Bubbles continue to grow and rise through the draft tube due to its buoyancy causing the bed particles to undergo in vigorous motion. This condition

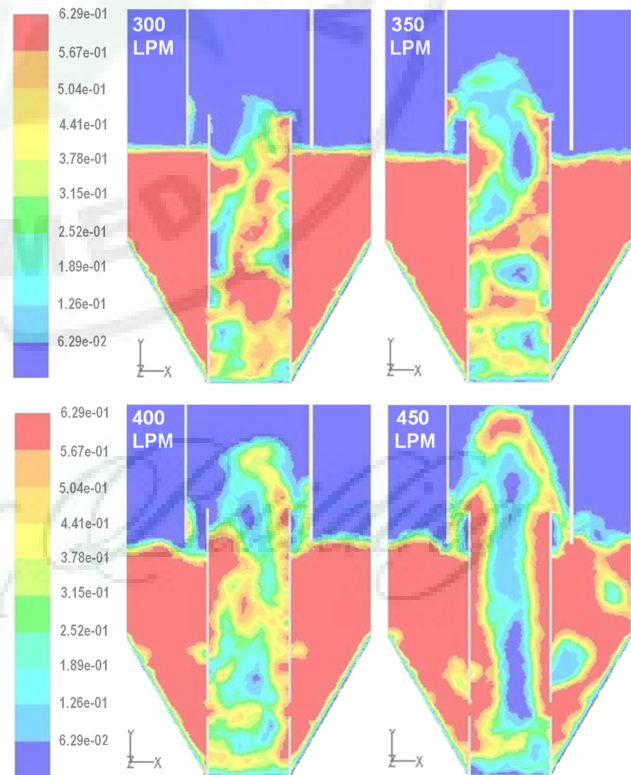


Fig. 3 Solid volume fraction contours at Qdt: 300–450 LPM (simulation group 1)

avored strong bed particle mixing and expanded beyond the top of the draft tube. The increase in bed material overflow from the top of the draft tube resulted in a decrease in solid volume fraction and also decrease in the bed pressure in the draft tube zone.

Consequently, pressure difference around the orifices increased resulting in more circulation.

By further increasing the fluidization flow rate into the draft tube above 350 LPM, the bed regime became highly turbulent and even behaved as spouted bed. This has caused a disturbance in the annulus zone as well and bubbles/voids started to form in the annulus. This is due to the high gas flow at the draft tube causing some gas to bypass from the draft tube into the annulus, and the annulus is no longer in the so-called aerated bed regime. For the ICFBG, bubbling fluidization in the annulus is undesirable as it dilutes the syngas with nitrogen causing a drop in its heating value. The bed pressures in the draft tube and the annulus are closely related to solid volume fractions. The pressure difference ( $\Delta P$ ) between the two zones provides a driving force for the solid and gas to flow from the annulus to the draft tube through the orifice.

**Effect of Air Flow Rate on Circulation.** In order to maintain the heat transfer between the gasification and combustion zones, bed material circulation rate must be maintained at a suitable rate. Aside from the geometry design parameters, air flow rate is the main operating variable that governs the pressure difference and circulation rate between the annulus and draft tube chambers.

Static bed pressures in the annulus and draft tube at the orifice level for simulation group 1 are shown in Fig. 4(a). The solid volume fractions in the bed correspond to the bed pressure. Therefore, increasing  $Q_{dt}$  resulted in a vigorous fluidization inside the draft tube creating low bulk density voids with considerable pressure drop caused by the sudden expansion of the voids. Consequently, the bed pressure in the draft tube was lower than that in the annulus and  $\Delta P$  increased through the whole  $Q_{dt}$  range from 300 LPM up to 450 LPM. Although  $\Delta P$  at the orifice increased almost linearly with the elevation of  $Q_{dt}$ ,  $G_s$  has shown a different pattern when changing the air flow supply. The effect of  $Q_{an}$  and  $Q_{dt}$  on  $G_s$  is shown in Fig. 4(b). Maximum circulation rate of 86.6 kg/h was achieved at  $Q_{dt}$  and  $Q_{an}$  of 350 and 150 LPM, respectively. In general, higher circulation can be achieved by increasing fluidization and aeration flow rates up to the optimum value where  $G_s$  starts to drop at higher air flow rate.  $Q_{dt}$  of 350 LPM presented the optimum fluidization flow where higher values caused gas bypass from the draft tube to the annulus resulting in a disturbance in material circulation as shown earlier in

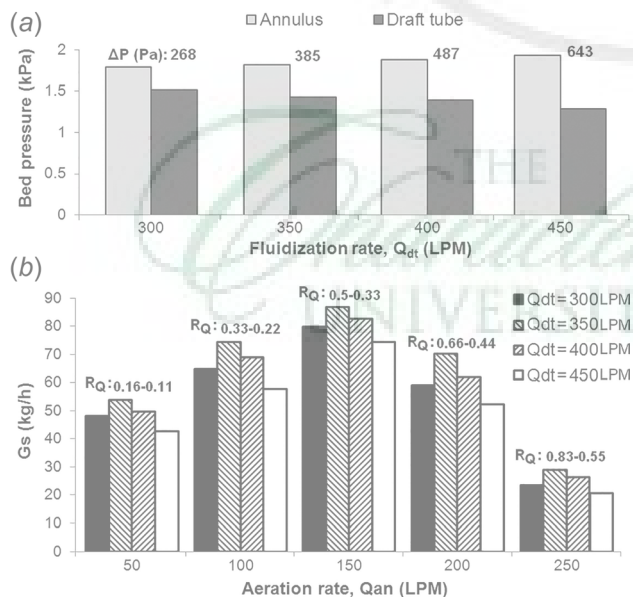


Fig. 4 Effect of (a)  $Q_{dt}$  on bed pressure and pressure difference (simulation group 1) and (b)  $Q_{an}$  and  $Q_{dt}$  on  $G_s$  (simulation groups 1 and 2)

Fig. 3. On the other hand,  $Q_{an}$  of 150 LPM presented the optimum aeration flow where higher values caused a fluidization in the annulus disturbing material circulation flow through the orifice holes.

$R_Q$  can be considered as a good indicator that combines the effect of  $Q_{an}$  and  $Q_{dt}$  on circulation. However,  $R_Q$  values are not conclusive and both  $Q_{an}$  and  $Q_{dt}$  have to be within the acceptable air flow range to achieve acceptable prediction of the circulation quality. For example,  $R_Q$  of 0.55 resulted in the lowest  $G_s$  of 20.6 kg/h at  $Q_{an}$  and  $Q_{dt}$  of 250 and 450 LPM, respectively. On the other hand, high  $G_s$  value of 80 kg/h was achieved at  $Q_{an}$  and  $Q_{dt}$  of 150 and 300 LPM, respectively, with  $R_Q$  of 0.5. In general, high circulation rates above 70 kg/h were achieved in the  $R_Q$  range of 0.28–0.57.

### Effect of the Static Bed Height

The initial level of bed material height ( $H_{bs}$ ) although is a geometry parameter, it is not permanent and can be varied even after the fabrication of the final design of the reactor. However, it is not as flexible as the operating variables and requires a disassembly of the ICFBG to change the bed height. Four  $H_{bs}$  values of 260, 280, 300, and 320 mm corresponding to 81.25%, 87.5%, 93.75%, and 100% of the draft tube height of 320 mm were considered as shown in Fig. 5(a). The results showed that an optimum bed height value can be identified although the circulation was heavily influenced by the air flow rates. Filling the bed materials to the top of the draft tube (i.e.,  $H_{bs} = H_{dt}$ ) resulted in the lowest  $G_s$  since the bed height at annulus was at the same plane level with no barrier to prevent back flow from the annulus to the draft tube. Maximum circulation was achieved when  $H_{bs}$  was 87.5% of  $H_{dt}$  reaching the dipleg bottom as shown in Fig. 5(b). Acceptable circulation rates were also achieved with further drop in the height down to 81.25% of  $H_{dt}$ , although the bed material level was below the dipleg bottom allowing gas bypass to the annulus which is not desirable.

**Effect of the Orifice Diameter.** The solid circulation mechanism depends mainly on the pressure difference between the two chambers. And since the bed pressure at the base of the draft tube is lower than that at the base of the annulus, some of the inlet air to the annulus tends to bypass to the draft tube side along with the solid. However, if the opening between the two chambers is large, reverse air bypassing from the draft tube to annulus is also possible. Therefore, orifice diameter plays a crucial role in controlling the circulation mechanism. The number of holes was limited to 8, thus, orifice diameter governs the solid flow just like in a flow

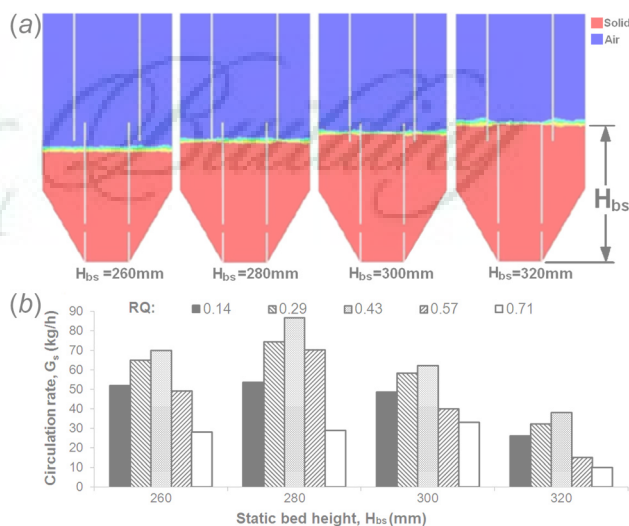


Fig. 5 (a) Contour of solid fraction initial condition on X-Y planes and (b) effect of  $H_{bs}$  on  $G_s$  (simulation group 3)

control valve. Varying  $D_{or}$  from 10 to 20 mm showed a significant elevation in  $G_s$  of more than twelve-fold increase as shown in Fig. 6(a). For small diameters, solid is clustered at the annulus near the orifices slowing the circulation process and opposing the air by pass to the draft tube. Increasing orifice diameter makes the solid clustering less severe and allowing for higher velocity through the orifice that enhances the orifice effect and increases pressure drop after the orifice. However, large diameters above 20 mm resulted in considerable flow disturbance with waves of back flow caused by the fluidization phenomenon inside the draft tube resulting in a significant drop in  $G_s$ . The graph also shows that the minimum  $D_{or}$  resulted in extreme reduction in circulation down to 9 kg/h for all  $R_Q$  ratios.

**Effect of the Inner Diameter of the Draft Tube.** With a fixed reactor diameter, draft tube diameter showed a considerable effect on circulation as shown in Fig. 6(b). By increasing or decreasing  $D_{dt}$ , the cross-sectional area of both the annulus and the draft tube also increases or decreases accordingly. Thus, larger  $D_{dt}$  resulted in larger quantity of solids into the draft tube, which require higher gas flow rate that increases the bed density in the annulus. Consequently, vigorous collisions occurred among the particles in the draft tube resulting in a drop in the gas flow to the annulus, while the gas flow to the draft tube increased. Optimum  $G_s$  occurred at  $D_{dt}$  of 125 mm that presented the optimum balance in cross section area and solid bed amount between annulus and draft tube.

**Effect of the Draft Tube Height.** The effect of the draft tube height on circulation is directly influenced by the static bed height as discussed earlier. And since the difference between two heights will increase by increasing tube height, bed height effect was neutralized by always changing it to the optimum value of 78.5% of  $H_{dt}$ . Extreme draft tube height of 370 mm has shown no circulation at all. By examining the pressure profile plot, it was found that the high back pressure inside the draft tube caused by the extra sand bed height has severely affected the pressure drop at the orifice. There was no crossover between the annulus and draft tube pressure lines as shown in Fig. 7(a). This means that the pressure inside the tube was higher than that in the annulus for all tube height and solid circulation was not possible. The effect of varying  $H_{dt}$  in the range of 260–350 mm on  $G_s$  is shown in Fig. 7(b). Reducing the tube height has improved the circulation

significantly, and at the height range of 280–320 mm, the circulation characteristics and pressure profile were almost similar to the optimum profile. Further reduction in the tube height down to 260 mm while maintaining the optimum fluidization flow of 350 LPM resulted in vigorous and disturbed fluidization inside the tube due to the lower bed weight. Moreover, air bypass from the draft tube to the annulus caused fluidization in the annulus even at low aeration flow causing significant reduction in circulation rate.

### Validation of Computer Simulation Using Experimental Simulation

In this work, the modeling was verified and validated using an experimental model in terms of bed material circulation. During the experiment, it was observed that the bed material circulation was not able to initiate below  $Q_{an}$  of 50 LPM. By increasing both  $Q_{an}$  and  $Q_{dt}$ , it was found that bed material circulation shown in Fig. 8(a) has followed similar trend to that established in the CFD simulation shown earlier in Fig. 4(b).

No bubbles occurred in the annulus zone until the fluidization to the draft tube reached 400 LPM and increased considerably at 450 LPM as confirmed earlier in Fig. 3. Circulation of bed materials improved significantly once  $Q_{an}$  and  $Q_{dt}$  were increased up to the optimum values of 150 and 350 LPM, respectively, followed by a drop and disturbance in the circulation at higher flow rates.

The  $G_s$  results for the optimum operating conditions obtained from CFD simulation were compared to the experimental model as shown in Fig. 8(b). Maximum circulation rate for the optimum operation with  $Q_{dt}$  and  $Q_{an}$  of 350 and 150 LPM, respectively, was in a good agreement with the experimental result with error margin below 5%. Higher error up to 10% was noticed at the extreme operating conditions and vigorous fluidization where the laminar flow setup might not be sufficient. In general, the CFD simulation tended to overpredict the circulation rate. This can be due to the ideal setup where the sand particle diameter and density were set as constants with a uniform bed distribution, whereas in the

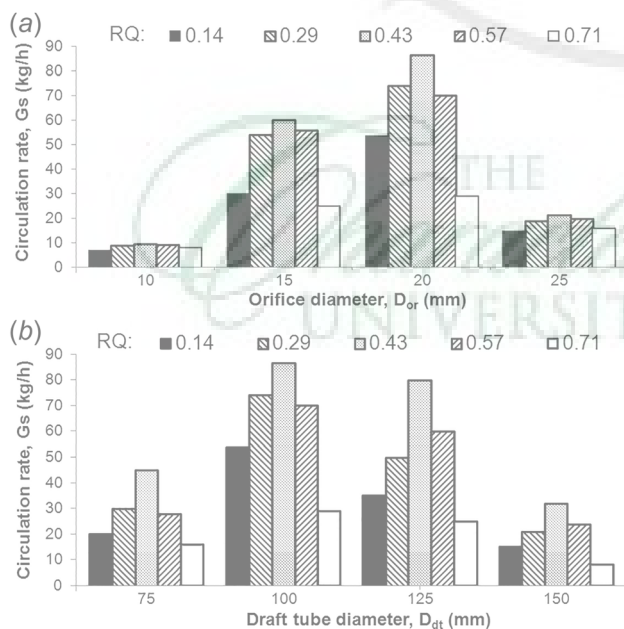


Fig. 6 Effect of (a)  $D_{or}$  on  $G_s$  (simulation group 5) and (b)  $D_{dt}$  on  $G_s$  (simulation group 4)

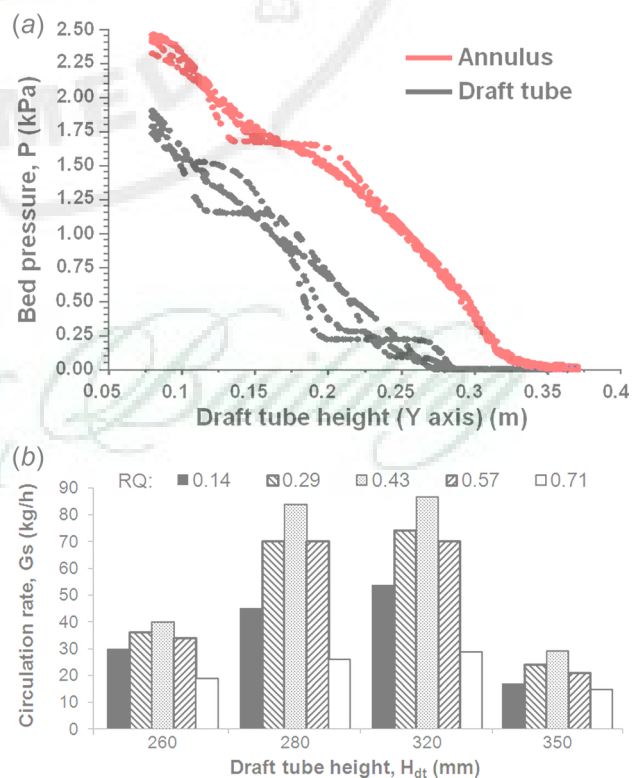
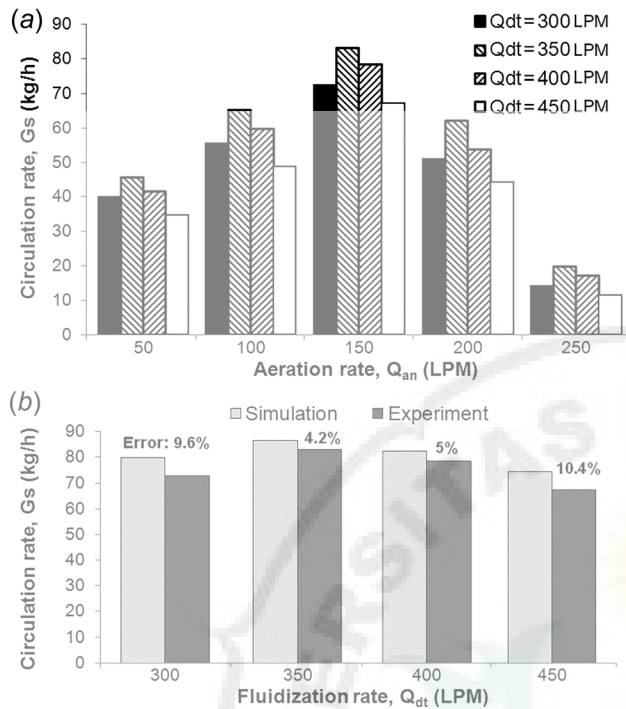


Fig. 7 (a) Bed pressure profile at  $H_{dt}$  of 370 mm and (b) effect of  $H_{dt}$  on  $G_s$  (simulation group 6)



**Fig. 8** (a) Effect of  $Q_{dt}$  and  $Q_{an}$  on  $G_s$  in the experimental model and (b) a comparison between the CFD simulation and experimental model (simulation group 1)

experiment the particles diameter ranged from 425 to 600  $\mu\text{m}$ . This can affect the actual friction and flow behavior of the bed especially at the extreme conditions.

## Conclusions

The hydrodynamic gas–solid flow in the ICFBG reactor was investigated using the Eulerian–Eulerian model with kinetic theory of granular flow. Two operating parameters,  $Q_{dt}$  and  $Q_{an}$ , governing the air flow to the reactor and four geometry parameters,  $H_{bs}$ ,  $H_{dt}$ ,  $D_{dt}$ , and  $D_{or}$ , were varied and evaluated to obtain optimum reactor geometry and operating conditions. It was found that solid circulation mechanism depended mostly on  $\Delta P$  between the annulus and the draft tube at the orifice level. The pressure drop inside the draft tube was created mainly by the orifice effect and also the low pressure void pockets caused by fluidization inside the tube. Fluidization and aeration flow rates showed significant effect on pressure difference and circulation rate between the chambers, and the optimum  $Q_{dt}$  and  $Q_{an}$  values were 350 and 150 LPM, respectively. As for the geometry parameters,  $D_{or}$  presented the most crucial variable with an optimum value of 20 mm, where a slight deviation from the optimum value affected the pressure drop inside draft tube significantly. The second geometry variable was  $H_{dt}$  where the tube height of 320 mm presented the optimum value while higher value of 370 mm resulted in no circulation at all. Other geometry variables with less effect on circulation were  $H_{bs}$  and  $D_{dt}$  with optimum values of 280 and 100 mm, respectively. The CFD simulation was validated and the solid circulation mechanism was visually observed and studied using full-scale plexiglass cold flow experimental model. The maximum  $G_s$  value of 86.6 kg/h obtained from simulation for the optimum geometry and operating conditions was in a good agreement with the experimental model with less than 5% deviation.

## Acknowledgment

The authors would like to thank the Universiti Sains Malaysia (RU I grant number: 814282) for the financial support of this study.

## Funding Data

- Universiti Sains Malaysia (RUI: 814282).

## Nomenclature

- $A_o$  = orifice area ( $\text{m}^2$ )
- $e_{ss}$  = coefficient of restitution
- $d_p$  = particle diameter ( $\mu\text{m}$ )
- $D_{dt}$  = draft tube diameter (mm)
- $D_{or}$  = draft tube orifice (mm)
- $G_s$  = solid circulation rate (kg/h)
- $H_{dt}$  = draft tube height (mm)
- $H_{bs}$  = bed static height (mm)
- $Q_{an}$  = aeration flow rate (LPM)
- $Q_{dt}$  = fluidization flow rate (LPM)
- $R_Q$  = fluidization rate

## References

- Ren, X., Meng, X., Panahi, A., Rokni, E., Sun, R., and Leventis, Y. A., 2018, "Hydrogen Chloride Release From Combustion of Corn Straw in a Fixed Bed," *ASME J. Energy Resour. Technol.*, **140**(5), p. 051801.
- Wladyslaw, M., 2017, "Co-Combustion of Pulverized Coal and Biomass in Fluidized Bed of Furnace," *ASME J. Energy Resour. Technol.*, **139**(6), p. 062204.
- Hassan, B., Ogidiana, O. V., Khan, M. N., and Shamim, T., 2017, "Energy and Exergy Analyses of a Power Plant With Carbon Dioxide Capture Using Multi-stage Chemical Looping Combustion," *ASME J. Energy Resour. Technol.*, **139**(3), p. 032002.
- Breault, R. W., Weber, J., Straub, D., and Bayham, S., 2017, "Computational Fluid Dynamics Modeling of the Fuel Reactor in NETL's 50 kWth Chemical Looping Facility," *ASME J. Energy Resour. Technol.*, **139**(4), p. 042211.
- Yan, Y., Feng, S., Zhang, L., Li, L., Zhang, L., and Yang, Z., 2018, "Experimental Research on Catalytic Combustion Characteristics of Inferior Coal and Sludge Mixture," *ASME J. Energy Resour. Technol.*, **140**(3), p. 032201.
- Sang, Z., Bo, Z., Liu, X., and Weng, Y., 2017, "Characteristic Analysis of a Rotary Regenerative Type Catalytic Combustion Reactor for Ultra Low Calorific Value Gas," *ASME J. Energy Resour. Technol.*, **139**(6), p. 062208.
- Lin, J.-C. M., 2007, "Combination of a Biomass Fired Updraft Gasifier and a Stirling Engine for Power Production," *ASME J. Energy Resour. Technol.*, **129**(1), pp. 66–70.
- Zhao, Y., Feng, D., Zhang, Z., Sun, S., Che, H., and Luan, J., 2018, "Experimental Study on Autothermal Cyclone Air Gasification of Biomass," *ASME J. Energy Resour. Technol.*, **140**(4), p. 042001.
- Kreitzberg, T., Hausteiner, H. D., Gövert, B., and Kneer, R., 2016, "Investigation of Gasification Reaction of Pulverized Char Under  $\text{N}_2/\text{CO}_2$  Atmosphere in a Small-Scale Fluidized Bed Reactor," *ASME J. Energy Resour. Technol.*, **138**(4), p. 042207.
- Guell, B. M., Sandquist, J., and Sörum, L., 2013, "Gasification of Biomass to Second Generation Biofuels: A Review," *ASME J. Energy Resour. Technol.*, **135**(1), p. 014001.
- Zainal, Z. A., Lahijani, P., Mohammadi, M., and Mohamed, A., 2010, "Gasification of Lignocellulosic Biomass in Fluidized Beds for Renewable Energy Development: A Review," *Renewable Sustainable Energy Rev.*, **14**(9), pp. 2852–2862.
- Zhou, Z., Ma, L. L., Yin, X. L., Wu, C. Z., Huang, L. C., and Wang, C., 2009, "Study on Biomass Circulation and Gasification Performance in a Clapboard-Type Internal Circulating Fluidized Bed Gasifier," *Biotechnol. Adv.*, **27**(5), pp. 612–615.
- Xiao, X., Le, D. D., Morishita, K., Zhang, S., Li, L., and Takarada, T., 2010, "Multi-Stage Biomass Gasification in Internally Circulating Fluidized-Bed Gasifier (ICFG): Test Operation of Animal-Waste-Derived Biomass and Parametric Investigation at Low Temperature," *Fuel Process. Technol.*, **91**(8), pp. 895–902.
- Barisano, D., Canneto, G., Nanna, F., Alvino, E., Pinto, G., Villone, A., Carnevale, M., Valerio, V., Battafarano, A., and Braccio, G., 2016, "Steam/Oxygen Biomass Gasification at Pilot Scale in an Internally Circulating Bubbling Fluidized Bed Reactor," *Fuel Process. Technol.*, **141**, pp. 74–81.
- Svoboda, K., Kalisz, S., Miccio, F., Wieczorek, K., and Pohorel, M., 2009, "Simplified Modeling of Circulating Flow of Solids Between a Fluidized Bed and a Vertical Pneumatic Transport Tube Reactor Connected by Orifices," *Powder Technol.*, **192**(1), pp. 65–73.
- Miccio, F., Ruoppolo, G., Kalisz, S., Andersen, L., Morgan, T. J., and Baxter, D., 2012, "Combined Gasification of Coal and Biomass in Internal Circulating Fluidized Bed," *Fuel Process. Technol.*, **95**, pp. 45–54.
- Simanjuntak, J. P., and Zainal, Z. A., 2015, "Experimental Study and Characterization of a Two-Compartment Cylindrical Internally Circulating Fluidized Bed Gasifier," *Biomass Bioenergy*, **77**, pp. 147–154.
- Jeon, J. H., Kim, S. D., Kim, S. J., and Kang, Y., 2008, "Solid Circulation and Gas Bypassing Characteristics in a Square Internally Circulating Fluidized Bed With Draft Tube," *Chem. Eng. Process.*, **47**(12), pp. 2351–2360.
- Zhao, W., Wang, T., Wang, C., and Sha, Z., 2013, "Hydrodynamic Behavior of an Internally Circulating Fluidized Bed With Tubular Gas Distributors," *Particulateology*, **11**(6), pp. 664–672.

- [20] Li, P., Yu, X., Liu, F., and Wang, T., 2015, "Hydrodynamic Behaviors of an Internally Circulating Fluidized Bed With Wide-Size-Distribution Particles for Preparing Polysilicon Granules," *Powder Technol.*, **281**, pp. 112–120.
- [21] Song, Y., Lu, X., Wang, Q., Li, J., Sun, S., Zheng, X., Yang, F., and Fan, X., 2017, "Experimental Study on Gas-Solid Flow Characteristics in an Internally Circulating Fluidized Bed Cold Test Apparatus," *Adv. Powder Technol.*, **28**(9), pp. 2102–2109.
- [22] Solnordal, C. B., Kenche, V., Hadley, T. D., Feng, Y., Witt, P. J., and Lim, K. S., 2015, "Simulation of an Internally Circulating Fluidized Bed Using a Multiphase Particle-in-Cell Method," *Powder Technol.*, **274**, pp. 123–134.
- [23] Lee, J. L., and Lim, E. W., 2017, "Comparisons of Eulerian-Eulerian and CFD-DEM Simulations of Mixing Behaviors in Bubbling Fluidized Beds," *Powder Technol.*, **318**, pp. 193–205.
- [24] Zhou, L., Zhang, L., Shi, W., Agarwal, R., and Li, W., 2018, "Transient Computational Fluid Dynamics/Discrete Element Method Simulation of Gas-Solid Flow in a Spouted Bed and Its Validation by High-Speed Imaging Experiment," *ASME J. Energy Resour. Technol.*, **140**(1), p. 012206.
- [25] Luo, K., Fang, M., Yang, S., Zhang, K., and Fan, J., 2013, "LES-DEM Investigation of an Internally Circulating Fluidized Bed: Effects of Gas and Solid Properties," *Chem. Eng. J.*, **228**, pp. 583–595.
- [26] Feng, Y., Smith, T. S., Witt, P. J., Doblin, C., Lim, S., and Schwarz, M. P., 2012, "CFD modeling of Gas-Solid Flow in an Internally Circulating Fluidized Bed," *Powder Technol.*, **219**, pp. 78–85.
- [27] Li, P., Wang, T., Liu, Y., Zhang, Q., Li, Q., Xiong, R., Guo, L., and Song, J., 2017, "CFD Simulation of the Hydrodynamic Behavior in an Internally Circulating Fluidized Bed Reactor for Producing Polysilicon Granules," *Powder Technol.*, **311**, pp. 496–505.
- [28] Juhui, C., Weijie, Y., Shuai, W., Guangbin, Y., Jiuru, L., Ting, H., and Feng, L., 2017, "Modelling of Coal/Biomass Co-Gasification in Internal Circulating Fluidized Bed Using Kinetic Theory of Granular Mixture," *Energy Convers. Manage.*, **148**, pp. 506–516.

